

UC Office of the President

Recent Work

Title

Locating the Source of Events in Power Distribution Systems Using Micro-PMU Data

Permalink

<https://escholarship.org/uc/item/4df4s0v5>

Journal

IEEE Transactions on Power Systems, 33(6)

ISSN

0885-8950 1558-0679

Authors

Farajollahi, Mohammad
Shahsavari, Alireza
Stewart, Emma M
[et al.](#)

Publication Date


2018-11-01

DOI

10.1109/TPWRS.2018.2832126

Peer reviewed

Locating the Source of Events in Power Distribution Systems Using Micro-PMU Data

Mohammad Farajollahi , *Student Member, IEEE*, Alireza Shahsavari, *Student Member, IEEE*, Emma M. Stewart, *Senior Member, IEEE*, and Hamed Mohsenian-Rad , *Senior Member, IEEE*

Abstract—A novel method is proposed to locate the source of events in power distribution systems by using *distribution-level phasor measurement units*, a.k.a., micro-PMUs. An event in this paper is defined rather broadly to include any major change in any component across the distribution feeder. The goal is to enhance *situational awareness* in distribution grid by keeping track of the operation (or misoperation) of various grid equipment, assets, distribution energy resources, loads, etc. The proposed method is built upon the *compensation theorem* in circuit theory to generate an equivalent circuit to represent the event by using voltage and current synchrophasors that are captured by micro-PMUs. Importantly, this method makes critical use of not only magnitude but also synchronized *phase angle* measurements, thus, it justifies the need to use micro-PMUs, as opposed to ordinary RMS-based voltage and current sensors. The proposed method can work with data from as a few as *only two* micro-PMUs. The effectiveness of the developed method is demonstrated through computer simulations on the IEEE 123-bus test system, and also on micro-PMUs measurements from a *real-life 12.47 kV test feeder* in Riverside, CA. The results verify that the proposed method is accurate and robust in locating the source of different types of events on power distribution systems.

Index Terms—Distribution synchrophasors, micro-PMUs, event source location, power quality and reliability events, data-driven method, compensation theorem, measurement differences.

I. INTRODUCTION

DISTRIBUTION-LEVEL phasor measurement units (PMUs), a.k.a., micro-PMUs (μ PMUs), have recently been introduced as new sensor technologies to enhance real-time monitoring in power distribution systems. Micro-PMUs provide GPS-synchronized measurements of three-phase voltage and current phasors at a high resolution, 120 readings per second [1]. Several emerging applications of micro-PMUs, including model validation, distribution system state estimation, topology detection, phase identification, distributed generation,

Manuscript received August 17, 2017; revised January 2, 2018, March 7, 2018, and April 23, 2018; accepted April 28, 2018. Date of publication May 1, 2018; date of current version October 18, 2018. This work was supported in part by NSF under Grants ECCS 1462530 and 1253516, in part by DoE under Grant EE 0008001, and in part by UCOP under Grant LFR-18-548175. Paper no. TPWRS-01289-2017. (*Corresponding author: Hamed Mohsenian-Rad.*)

M. Farajollahi, A. Shahsavari, and H. Mohsenian-Rad are with the Department of Electrical and Computer Engineering, University of California, Riverside, CA 92521 USA (e-mail: mfara006@ucr.edu; ashah023@ucr.edu; hamed@ece.ucr.edu).

E. Stewart is with the Infrastructure Systems, Cyber and Physical Resilience, Lawrence Livermore National Laboratory, Livermore, CA 94550 USA.

Color versions of one or more of the figures in this paper are available online at <http://ieeexplore.ieee.org>.

Digital Object Identifier 10.1109/TPWRS.2018.2832126

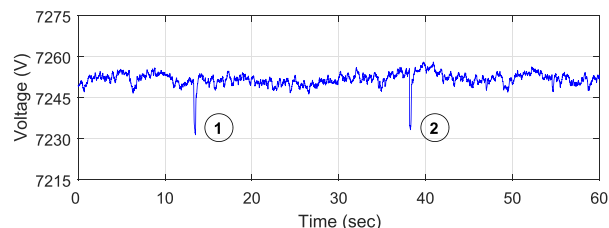


Fig. 1. Voltage phasor magnitude that is measured in a distribution substation in Riverside, CA. Only one phase is shown here. Event 1 has a root cause in the transmission system. Event 2 has a root cause in the distribution system.

and transient analysis, as discussed in a recent survey in [2] and the references therein.

A. Motivation

Consider one minute of voltage phasor measurements in Fig. 1 from a micro-PMU at a real-life 12.47 kV distribution substation in Riverside, CA. As expected, there are fluctuations in voltage magnitude, including two voltage sag events. Each event has a *root cause* at either transmission network or distribution network [3]. Common root causes of distribution level events include load switching, capacitor bank switching, connection or disconnection of distributed energy resources (DERs), inverter malfunction, a minor fault, etc. Accordingly, in this paper, we seek to answer the following question: *for those events with root causes in distribution network, what is the location of such root cause, i.e., at what exact distribution bus does the load switching, capacitor bank switching, DER connection/disconnection, or device malfunction occur?*

Answering the above question is the key to achieving *situational awareness* in power distribution systems, so as to keep track of how various grid equipment, assets, DERs, and loads operate or misoperate. The applications are diverse, ranging from identifying incipient failures [1], [4] or cyber-attacks [5], to recruiting demand side resources to construct a self-organizing power distribution system [6]–[8]. Here, an *event* is defined rather broadly to include any major change in a component across the distribution feeder. This of course includes the two traditional classes of electric distribution system events, namely *power quality (PQ)* events, such as dropping below or exceeding above acceptable nodal voltage limits, as well as *reliability* events, such as interrupting service due to faults that cause fuse blowing or relay tripping [9]. However, since the goal in this paper is to enhance *situational awareness* in power distribution systems, we are interested also in PQ events that do not necessarily violate PQ requirements or undermine reliability, but they

do indicate *how different components across the distribution feeder operate*.

B. Related Work

Considering the related literature on micro-PMUs, so far, most studies have focused on detecting the presence of and/or scrutinizing the characteristics of certain events, *whose source locations are assumed to be known*. The events that have been previously studied include capacitor bank switching [4], transformer tap changing [10], inverter misoperation [11], and load switching [6]. Importantly, the above studies are *complementary* to what we do in this paper, because once the source of an event is located by using the proposed method in this paper, one can use the techniques in [4], [6], [10], [11] to further the event and its characteristics.

There are also occasional studies that address event source location identification using micro-PMUs such as [12], [13]. High-impedance fault location identification is reported [14].

As for the general literature on event source location identification, it is rich; *however, most prior studies are not related to micro-PMUs*. Several methods in this field can be classified as *impedance-based* methods, which work based on calculating the impedance between the event location and the sensor location. These methods are widely used to locate *permanent faults* [15], [16]. A fundamental assumption in impedance-based methods is that the change in impedance is purely resistive. However, this assumption is not true in events such as DER switching, capacitor bank switching, and load switching. Therefore, impedance-based method cannot be directly applied for these types of events.

Another class of methods work based on *wide-area monitoring*. They collect and examine data from several sensors across the distribution system. Most existing wide-area monitoring methods are concerned only with *fault* events, e.g., in [17], [18]. They often work by first *hypothetically* placing the event at different locations, then calculating the states of the distribution system corresponding to each hypothesis, and then comparing the state calculation results with measurements to test each hypothesis. This can be computationally complex.

Wide-area methods are used also to identify the source location for major PQ events, e.g., in [19]; to obtain the operation status for DERs, e.g., in [20], [21]; and to detect islanding [22]. They often use state or parameter estimation or other statistical techniques. Therefore, they may need several sensors in order to assure accuracy, as opposed to as few as only two sensors in this paper. Also, it is common for this group of methods to use *waveform sensors*, as opposed to micro-PMUs, to compare the voltage and/or current waveforms at different locations.

C. Summary of Technical Contributions

This paper proposes a novel method to locate the source of events in power distribution systems, where *events* are defined in a broad sense as in Section I-A. The main technical contributions in this paper can be summarized as follows:

- 1) The proposed method is developed based on the *compensation theorem* in circuit theory to generate an *equivalent circuit* to represent the event by using voltage and current synchrophasor measurements. Our method does *not* require making any hypothesis about the location of the

event. It locates the source of the event rather *directly* and by solving an optimization problem. The source location of all events are identified using micro-PMUs, as opposed to waveform sensors, see Section I-B.

- 2) The proposed method can utilize data from as few as *only two* micro-PMUs, that are installed at the beginning and at the end of a feeder, to locate the source of an event, *anywhere along the main feeder*, see Section II. If additional micro-PMUs are available also at the end of the laterals, then our method can pinpoint the event source location *also along the laterals*, see Section III.
- 3) The proposed method makes critical use of not only magnitude measurements but also *phase angle measurements* that are obtained by micro-PMUs. This is an important feature, because so far, the role of phase-angle measurements is still not fully understood in many applications in the literature on micro-PMUs. The importance of using phase angle measurements is discussed both *analytically*, see Section IV, and through case studies.
- 4) The proposed method works based on *measurement differences*. This feature can help alleviate constant errors in *instrumentation channel*, such as errors at current transformers (CTs) and potential transformers (PTs), which are often orders of magnitude higher than the errors in the micro-PMU device itself. As a result, the performance of the proposed method is robust with respect to typical measurement errors.

II. EVENT SOURCE LOCATION IDENTIFICATION METHOD

This section describes the proposed method for locate the source of an event in a distribution feeder. Throughout this section we assume that exactly two micro-PMUs are installed on the feeder. The extension to the case with several micro-PMUs will be discussed later in Section III.

A. Background: Compensation Theorem

An event in an electric circuit can change all or a subset of nodal voltages and branch currents along the circuit. According to the *compensation theorem* [23, pp. 177], once an element changes in a circuit, the amount of changes in nodal voltages and branch currents can be obtained through an *equivalent circuit*. In such equivalent circuit, the element that has changed is replaced with a current source that injects current at a level equal to the amount of change in the current going through the element; and all sources are *replaced* with their internal impedances.

The importance of the compensation theorem in this paper is that the analysis of an event through equivalent circuit is easier than through the original circuit.

An example is shown in Fig. 2. The event in this example is a change in impedance Z . The pre-event impedance is denoted by Z^{pre} , as in Fig. 2(a). The post-event impedance is denoted by Z^{post} , as in Fig. 2(b). Let I^{pre} and I^{post} denote the current drawn by the element *before* and *after* the event, respectively. Based on the compensation theorem, the equivalent circuit of this network can be obtained by replacing the impedance element that caused the event with current source

$$\Delta I = I^{\text{post}} - I^{\text{pre}}, \quad (1)$$

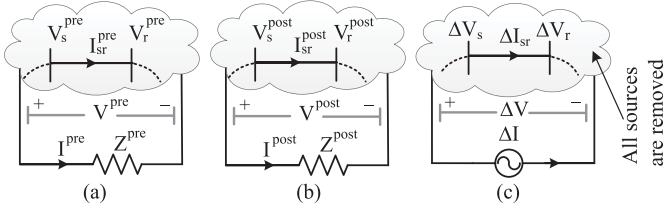


Fig. 2. An illustration of compensation theorem. (a) Pre-event network. (b) Post-event network. (c) Equivalent circuit based on compensation theorem.

and all sources with their internal impedances. The equivalent network, shown in Fig. 2(c), can then be used to analyze the changes of the nodal voltages and branch currents:

$$\Delta V_s = V_s^{\text{post}} - V_s^{\text{pre}}, \quad (2)$$

$$\Delta I_{sr} = I_{sr}^{\text{post}} - I_{sr}^{\text{pre}}, \quad (3)$$

where subscriptions s and r denote two arbitrary neighboring nodes. Next, we propose a novel application of the compensation theorem to help locate the source of events.

B. Pre-Step: Event Detection

Before identifying the location of an event, we must first become aware of the occurrence of such event. Thanks to the recent advances in applying data-driven techniques to micro-PMU data, there already exist effective methods to detect the presence of the event, e.g., see [24], [25]. The event detection process is continuously carried out based on such algorithms. Once the occurrence of an event is detected, the next step is to use an algorithm that can identify the location of the root cause of the event; as we will describe next.

C. Step 1: Identifying the Region of the Event Source

Consider a distribution feeder, such as in Fig. 3. Suppose two micro-PMUs are installed on this feeder. There are n buses between the two micro-PMUs. These buses may or may not have laterals. The voltage and current at the downstream and upstream of the feeder are recorded by the two micro-PMUs. An event may occur in one of the following three regions:

- upstream of micro-PMU u ,
- downstream of micro-PMU d ,
- between micro-PMU u and micro-PMU d .

In order to determine the region of the event source, next, we define the equivalent upstream impedance of the feeder seen by micro-PMU u and the equivalent downstream impedance of the feeder seen by the micro-PMU d as:

$$Z^u \triangleq \frac{\Delta V^u}{\Delta I^u} \quad (4)$$

$$Z^d \triangleq \frac{\Delta V^d}{\Delta I^d}, \quad (5)$$

respectively, where ΔV^u and ΔV^d indicate the difference between the pre-event and post-event voltage phasors, captured by micro-PMUs u and d . Also, ΔI^u and ΔI^d denotes the difference in current phasors, captured by these micro-PMUs. Note that the direction of current that is measured by the two micro-PMUs is the opposite of each other, as shown in Fig. 3; micro-PMU

u measures the current flowing towards upstream, i.e., to the left, while micro-PMU d measures the current flowing towards downstream, i.e., to the right.

Based upon the analysis in [26], we argue that the *real* parts of Z^u and Z^d determine the region of the event source. If $\text{Real}\{Z^u\}$ is *negative*, then the event source is located in the upstream of micro-PMU u . Similarly, if $\text{Real}\{Z^d\}$ is *negative*, then the event source is located in the downstream of micro-PMU d . Finally, if $\text{Real}\{Z^u\}$ and $\text{Real}\{Z^d\}$ are both *positive*, then the event source is located between the two micro-PMUs.

Now, suppose micro-PMU u is installed at the *feeder-head* at the distribution substation. Also, suppose micro-PMU d is installed at the terminal bus, i.e., at the *end* of the feeder. In that case, if the region of the event source is the upstream of micro-PMU u , then the event has a root-cause outside the distribution feeder of interest, such as in the transmission system. If the region of the event source is the downstream of micro-PMU d , then the source is simply on the terminal bus. Therefore, *for the rest of this section, our focus is on locating the source of the event when it occurs somewhere across the distribution feeder, i.e., between the two micro-PMUs.*

D. Step 2: Forward Nodal Voltages Calculation

Suppose the event source is connected to bus k , where $k \in \{1, \dots, n\}$. Based on the compensation theorem, a current source with current ΔI_k can be placed at bus k to create an equivalent circuit. The nodal voltages and branch currents on this equivalent circuit at the buses where the two micro-PMUs are installed are equal to the *changes* in nodal voltages and branch currents, obtained as in (2) and (3), respectively.

Next, by using the measurements from micro-PMU u , together with pseudo-measurements, and by successively applying the Kirchhoff Voltage Law (KVL), we can obtain:

$$\begin{aligned} \Delta V_1^f &= \Delta V^u \\ \Delta V_2^f &= \Delta V_1^f + (\Delta I^u + \Delta I_1^f)Z_1 \\ &\vdots \\ \Delta V_n^f &= \Delta V_{n-1}^f + (\Delta I^u + \Delta I_1^f + \dots + \Delta I_{n-1}^f)Z_{n-1}, \end{aligned} \quad (6)$$

where ΔV_i^f denotes the calculated nodal voltage at bus i , and ΔI_i^f denotes the calculated current injection at bus i . Superscript f indicates the fact that the quantities are obtained using *forward calculation*. Without loss of generality, we assume that all loads are constant-impedance; hence the current injection at node i is calculated as

$$\Delta I_i^f = Y_i \Delta V_i^f, \quad (7)$$

where Y_i indicates the equivalent admittance of lateral i and is considered as pseudo-measurements. By replacing (7) in (6), one can start from the measurements of micro-PMU u and sequentially calculate $\Delta V_1^f, \Delta V_2^f, \dots, \Delta V_n^f$.

Other types of loads, namely constant-current and constant-power loads, can also be formulated and similarly integrated into the model using adequate pseudo-measurements. The impact of other types of load is discussed in the Appendix.

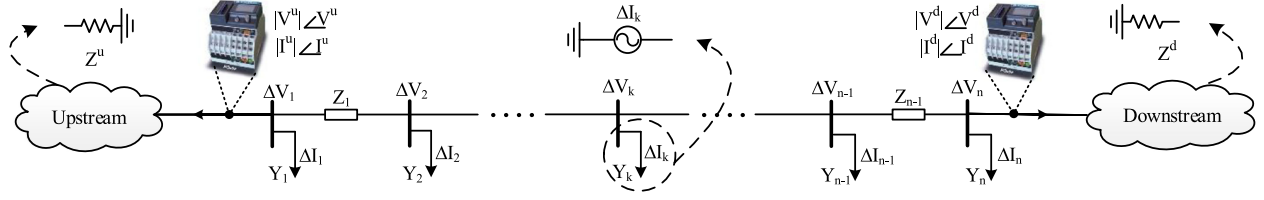


Fig. 3. Representation of a distribution feeder based on compensation theorem equivalent circuit. Measurements are done by two micro-PMUs.

E. Step 3: Backward Nodal Voltages Calculation

In a similar manner, we can start from sensor bus d , use the measurements of micro-PMU d , together with pseudo-measurements, and successively apply KVL in order to obtain:

$$\begin{aligned} \Delta V_n^b &= \Delta V^d \\ \Delta V_{n-1}^b &= \Delta V_n^b + (\Delta I^d + \Delta I_n^b)Z_{n-1} \\ &\vdots \\ \Delta V_1^b &= \Delta V_2^b + (\Delta I^d + \Delta I_n^b + \dots + \Delta I_2^b)Z_1, \end{aligned} \quad (8)$$

where superscript b indicates that the intended voltage or current phasor is obtained using *backward calculation*. Again, by assuming that all loads are constant-impedance, the current injection at node i is calculated as

$$\Delta I_i^b = Y_i \Delta V_i^b. \quad (9)$$

By replacing (9) in (8), one can start from micro-PMU d and sequentially calculate $\Delta V_n^b, \Delta V_{n-1}^b, \dots, \Delta V_1^b$.

F. Step 4: Voltage Comparison

In (6) and (8), it is assumed that at each bus the current injection can be obtained from the *production of nodal voltage and bus admittance*. This is a valid assumption at all buses, *except for bus k* in which the event occurs. Recall from the compensation theorem that at this bus, a current source injects ΔI_k into the equivalent circuit of the feeder and therefore, the production of voltage and bus admittance *is no longer a correct indication of the bus current*. As a result, we can make the following distinctions across the calculated nodal voltages:

$$\begin{aligned} &\underbrace{\{\Delta V_1^f, \dots, \Delta V_{k-1}^f, \Delta V_k^f, \Delta V_{k+1}^f, \dots, \Delta V_n^f\}}_{\text{correct}} \quad \underbrace{\{\Delta V_{k+1}^f, \dots, \Delta V_n^f\}}_{\text{incorrect}} \\ &\underbrace{\{\Delta V_1^b, \dots, \Delta V_{k-1}^b, \Delta V_k^b, \Delta V_{k+1}^b, \dots, \Delta V_n^b\}}_{\text{incorrect}} \quad \underbrace{\{\Delta V_{k+1}^b, \dots, \Delta V_n^b\}}_{\text{correct}}. \end{aligned} \quad (10)$$

The fundamental observation in (10) is that the calculated voltage at bus k in both backward and forward nodal voltage calculations is a *correct* value. In other words, ΔV_k^f and ΔV_k^b are essentially *equal*, because if they are not equal, then at least one of them must be incorrect, which is a contradiction.

Next, we define the *discrepancy* of the nodal voltages obtained from both calculations across all buses as:

$$\Phi_i = |\Delta V_i^f - \Delta V_i^b|, \quad \forall i, \quad (11)$$

where ΔV_i^f and ΔV_i^b are as in (6) and (8), respectively. From (10), among all buses, the voltage at bus k in the two nodal

Algorithm 1: ESLI with Two Micro-PMUs.

Input: Micro-PMUs measurements, pseudo-measurements.

Output: The location of the event source.

Pre-Step:

An event is detected.

Step1:

Obtain Z^u and Z^d , as in (4) and (5), respectively.

if $\text{Real}\{Z^u\} < 0$, **then**

The event source is outside the feeder of interest.

else if $\text{Real}\{Z^d\} < 0$, **then**

The event source is the terminal bus.

else

Step2:

Obtain ΔV_i^f using (6).

Step3:

Obtain ΔV_i^b using (8).

Step4:

Obtain Φ_i using (11).

Obtain the event source location k using (12).

return k

end if

voltage calculation methods must be almost equal; hence, it is expected that Φ_k has the *minimum* value among all buses. Therefore, the event source location can be obtained as:

$$k = \arg \min_i \Phi_i. \quad (12)$$

The proposed Event Source Location Identification (ESLI) method is summarized in Algorithm 1. First, the event is detected. Then, we use the method in Section II-C to identify the region of the event source. Algorithm 1 reaches a conclusion if the event source is outside of the feeder or at the terminal bus in Step1. Otherwise, it goes through the forward and backward nodal voltage calculations in Step2 and Step3, respectively. Then, the exact event source location is identified in Step4.

III. EXTENSION TO THE CASE WITH ARBITRARY NUMBER OF MICRO-PMUS

So far, we analyzed the case when only two micro-PMUs are available. In this section, we extend our method to incorporate the case with $m \geq 2$ micro-PMUs. Again, one micro-PMU is installed at the feeder-head to distinguish the events that are originated at the distribution system from those that are originated at the transmission system using the method in Section II-C. Other micro-PMUs are installed at the end of the main and a subset of laterals.

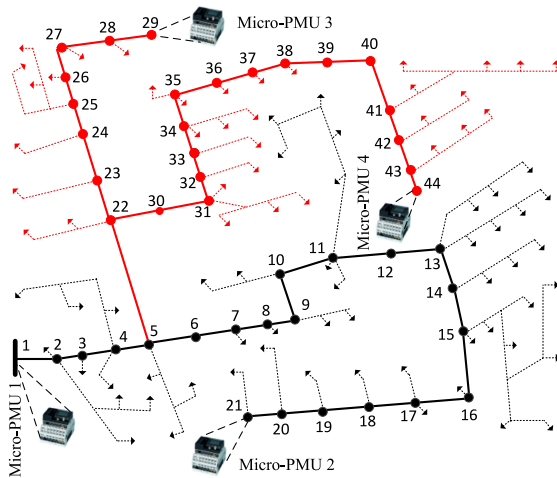


Fig. 4. The IEEE 123 bus test system equipped with 4 micro-PMUs. If only micro-PMUs 1 and 2 are available, then buses 1 to 21 become observable. The MST is shown with a tick black line in this case. If micro-PMUs 3 and 4 also become available, then buses 22 to 44 also become observable. The MST in this case is extended to include also the thick red line.

Next, we use the concept of *minimum spanning tree* (MST), which is defined as the path that connects all micro-PMUs across the distribution feeder. In order to create an MST in a distribution feeder, at least two micro-PMUs are required. Assume micro-PMUs 1 and 2 are installed on the IEEE 123 bus test system, as shown in Fig. 4.

The MST for this configuration includes the buses between these two micro-PMUs, i.e. buses 1 to 21. We refer to these buses as *MST buses*. The number of MST buses in this example is $n = 21$.

The location of an event is identified on MST buses, which indicates that the event has occurred either on the identified MST bus itself, or on a lateral that stems from this identified MST bus. For instance, if bus 16 is identified as the location of an event, then we are confident that the event has indeed occurred at this bus, because bus 16 does not have a lateral. However, if bus 5 is identified as the location of an event, then the actual event location could be bus 5 itself or somewhere on the lateral that stems from bus 5, i.e., buses 22 to 44 which are shown in red in Fig. 4. This issue can be resolved only if additional micro-PMUs are installed on this network. For instance, as shown in Fig. 4, we can increase the number of MST buses to $n = 29$, including buses 22 to 29, if we install micro-PMU 3 at bus 29. Similarly, by adding micro-PMU 4 at bus 44, we can turn buses 30 to 44 into MST buses.

In order to achieve full observability, i.e., to turn all buses into MST buses to identify the exact event bus location when it occurs wherever on any lateral, we must to install at least a total of *one plus the number of laterals* micro-PMUs; one at the substation and one at the end of each lateral. However, such full observability on each and every lateral may not be necessary in practice. In fact, in many cases it is sufficient to identify the lateral that hosts the event; rather than the exact bus on such identified lateral. For example, by increasing the number of micro-PMUs from 2 to 4 in Fig. 4, we can improve system observability by a great extent, which is sufficient for practical purposes to identify most major events.

Algorithm 2: ESLI with Multiple Micro-PMUs.

Same as in Algorithm 1, but replace Step4 with:

Step4:

- Obtain ΔV^j for any micro-PMU j similar to (6) and (8).
 - Obtain vector Φ using (13).
-

To obtain an alternative and more systematic approach, let ΔV_i^j denote the voltage phasor of MST bus i that is calculated by using the measurements of micro-PMU j , together with pseudo-measurements, and by successively applying KVL starting from micro-PMU j in the equivalent circuit, just like what we did in (6) and (8). Next, as in Section II-F, we use the *discrepancy* among the calculated nodal voltage phasors based on all measurements from different micro-PMUs and obtain the event source location by solving the minimization in (12) but with the following updated objective function:

$$\Phi_i = \sum_{j=1}^{m-1} \sum_{s=j+1}^m \left| \Delta V_i^j - \Delta V_i^s \right|, \quad \forall i. \quad (13)$$

where m shows the number of micro-PMUs deployed across the power distribution system. Indexes j and s are associated with micro-PMUs $1, \dots, m$; and index i is associated with buses $1, \dots, n$ on the minimum spanning tree.

Specifically, for each *pair* of micro-PMUs j and s , the expression in (13) calculates the discrepancy of the nodal voltages obtained from the forward and backward calculations that starts from micro-PMU j and ends at micro-PMU s ; and vice versa. In other words, for a given pair of micro-PMUs j and s , the expression in (13) is identical to the expression in (11) in Section II-F. Accordingly, the expression in (13) simply repeats and combines such discrepancy calculations across *all possible pairs* of micro-PMUs j and s . The combination is achieved through the two summation operators in this equation. The rest of the analysis is exactly the same as in Section II. We can now update Algorithm 1 to cover the case with multiple micro-PMUs, as shown in Algorithm 2.

IV. IMPORTANCE OF MEASURING PHASE ANGLE

In this section, we discuss the importance of using not only magnitude measurements but also phase angle measurements that are obtained by micro-PMUs. The goal is to analytically examine the need for using an advanced sensor such as micro-PMU, as opposed to using ordinary RMS-value sensors.

Consider an event and suppose the changes in voltage at a given sensor location are captured by a micro-PMU as shown in Fig. 5(a). Suppose the event occurs on the upstream of the micro-PMU, as indicated by placing the current source on the left hand side of the micro-PMU in Fig. 5(a). Note that, the voltage difference ΔV^d is a phasor. It is obtained as

$$\Delta V^d = \frac{Z^u Z^d}{Z^u + Z^d} \Delta I^u = Z^{\text{eq}} \Delta I^u. \quad (14)$$

If we take the magnitude of ΔV^d as fixed, then the post-event phasor would vary on the dashed circle, changing angle α , as shown in Fig. 5(b). The exact value of α depends on the type of event, such as load switching, capacitor bank switching, DERs

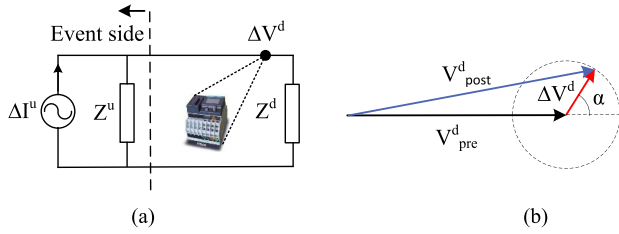


Fig. 5. The importance of measuring phase angles for phasors V_{pre}^d and V_{post}^d depends on angle α . (a) Equivalent circuit. (b) Voltage phasor diagram.

switching, faults, etc. We can show that

$$\alpha = \angle Z^{eq} + \angle \Delta I^u. \quad (15)$$

Note that, the cosine of $\angle Z^{eq}$ can be loosely interpreted as the *power factor* of the event-induced equivalent circuit.

If the phase angle difference α is exactly zero or 180° , i.e., if the post-event voltage phasor is in line with the pre-event voltage phasor, then it is sufficient to measure only the magnitude of voltage in order to use the analysis in this paper. From (15), for α to be zero or 180° , we must have either

$$\angle \Delta I^u = -\angle Z^{eq} \quad \text{or} \quad \angle \Delta I^u = \pi - \angle Z^{eq}. \quad (16)$$

In such special cases, one can use a standard RMS-based voltage sensor, as opposed to a micro-PMU, in order to identify the location of the event using our proposed method.

If neither of the conditions in (16) hold, then measuring phasor angle, i.e., the use of micro-PMUs, is necessary. However, the extent of such necessity depends on the value of α . Of interest are those events that only change the voltage phase-angle but not the voltage magnitude, i.e. when either

$$\alpha = \pi/2 + \arcsin(\Delta V^d/2V_{pre}^d) \quad (17)$$

$$\text{or } \alpha = -\pi/2 - \arcsin(\Delta V^d/2V_{pre}^d). \quad (18)$$

If any of the above conditions hold, then measuring voltage magnitude alone, such as by using standard RMS-based voltage sensors, is simply useless for the purpose of even location identification. One must use micro-PMUs instead.

In practice, we often have $\Delta V^d \ll V_{pre}^d$ for most PQ events. In that case, the arcsin terms in (17) and (18) would be negligible. From this, together with (15), we can approximate the conditions in (17) and (18) as $\angle \Delta I \approx -\angle Z^{eq} \pm \pi/2$.

We will further investigate the importance of measuring phase angles through multiple case studies in Section V-B.

V. CASE STUDIES: PART I - IEEE TEST NETWORK

Again consider the IEEE 123-bus test system in Fig. 4, where the parameters are as in [27]. This network has several laterals and sub-laterals, which feed different types of balanced and unbalanced loads. Four micro-PMUs are installed at buses 1, 21, 29, and 44, as marked in Fig. 4. The efficiency and robustness of the proposed ESLI method is tested on this network for several predefined event scenarios. In each scenario, the discrepancy measure Φ_k is calculated at each bus $k = 1, 2, \dots, 44$ by utilizing a three-phase load flow method in MATLAB for *pre-event* and *post-event* time-stamps.

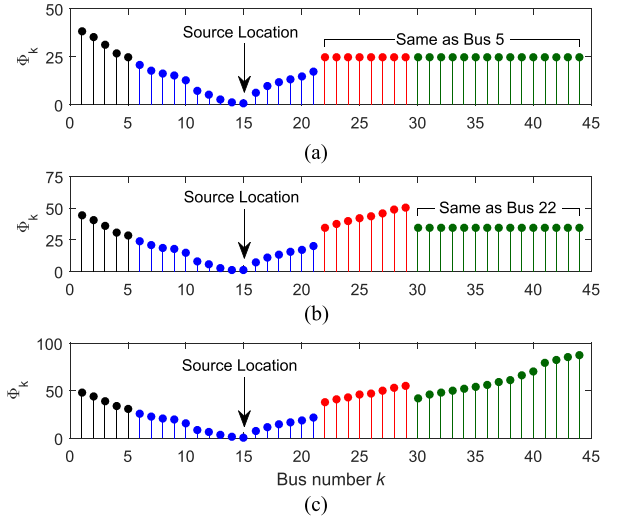


Fig. 6. Results for Case I based on the IEEE 123-bus test system, with data. (a) From two micro-PMUs. (b) From three micro-PMUs. (c) From four micro-PMUs.

A. Examining Four Different Event Scenarios

Case I - Capacitor Bank Switching at Bus 15: Capacitor bank switching is a persistent but minor PQ event in power distribution systems. Commonly, capacitor banks are switched by voltage regulated controllers. Since most capacitors do not have built-in monitoring systems, utilities need to perform manual patrol and inspections to verify proper operation of their capacitors or to identify any PQ event that is caused by any incipient failure with volt/var control switching [4]. Alternatively, we can use the proposed ESLI method to *remotely monitor* the operation of capacitor banks. As an example, suppose a 600 kVAR capacitor is switched off at bus 15. The ESLI algorithm is used to obtain Φ_k for $k = 1, 2, \dots, 44$ based on three different micro-PMUs data availability scenarios.

First, suppose data is available only from two micro-PMUs, i.e., micro-PMUs 1 and 2. The results are shown in Fig. 6(a). In this case, the MST includes buses 1 to 21. Since the location of the capacitor, i.e., bus 15, is on the MST, the event source location is correctly identified at the *minimum of the discrepancy bar chart* in Fig 6(a). Note that, since buses 22 to 44 are *not* MST buses due to the absence of micro-PMUs 3 and 4, they do not carry separate discrepancy measures; they rather take the same discrepancy measure as MST bus 5.

Second, suppose the data is available from Micro-PMUs 1, 2, and 3. In this case, the MST expands to include buses 22 to 29. The obtained results are presented in Fig. 6(b).

Finally, suppose the data is available from all four micro-PMUs. In that case, the MST includes all buses 1 to 44. The results are shown in Fig. 6(c). We can conclude that in Case I, the use of micro-PMUs 3 and 4 is not necessary, *because the MST already includes the event bus 15 even if only micro-PMUs 1 and 2 are available*. Although, having redundancy measurements could help if the measurements are noisy.

Case II - Load or DER Switching at Bus 24: Suppose a single-phase 40 kW + 20 kVAR load switches on at bus 24, causing a *small voltage sag*, see [6]. The source of such event can be *remotely* located using micro-PMU data. The results are

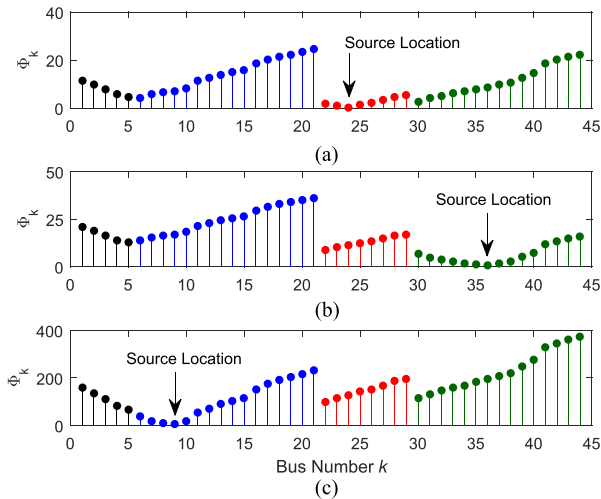


Fig. 7. Results for Cases II to IV based on the IEEE 123-bus test system, using data from four micro-PMUs. (a) Case II. (b) Case III. (c) Case IV.

shown in Fig. 7(a). The minimum of the discrepancy measure Φ_k provides the correct event source location at bus 24. Here, we assume that all four micro-PMUs are available. If micro-PMU 3 is not available, then bus 22 is selected as the event source location, because in that case bus 24 is not on the MST.

Case III - High Impedance Fault at Bus 36: High impedance faults may not interrupt service; but they must be identified to isolate the faulted area due to safety. Suppose a single-phase high impedance fault with 100Ω fault resistance occurs at bus 36. The results for this event are shown in Fig. 7(b). The event source location is *correctly* identified at bus 36.

Case IV - Low Impedance Fault at Bus 9: Low impedance faults are often reliability events which require operating the protection devices. Suppose a three-phase fault with 5Ω fault resistance occurs at bus 9. The results of applying the ESLI algorithm are shown in Fig. 7(c). Again, we can see that the minimum of the discrepancy measure Φ_k across $k = 1, \dots, 44$ correctly indicates the event source location at bus 9.

It is interesting to compare the extent of discrepancy value Case IV with those in Cases I and II, where the event was of minor PQ type. The discrepancy is much higher for the major reliability event in Case IV. That means, there is a much greater margin of accuracy in identifying the correct location for reliability events; therefore, it is less likely for the location of an reliability event to be identified incorrectly.

B. Importance of Using Phase Angle Measurements

Recall from Section IV that the importance of using phase angle measurements for the analysis in this paper depends on the angle α that the event creates between V_{pre}^d and V_{post}^d , see Fig. 5(b). In this section, we compare two cases, namely Case A and Case B, to further explain this concept. Without loss of generality, suppose only two micro-PMUs, i.e., micro-PMUs 1 and 2 are available. The two events are defined as follows:

- *Case A:* A 40 kW + 80 kVAR load is switched on at bus 11. This results in $V_{pre}^d = 2332.1 \angle 5.1183^\circ$ and $V_{post}^d = 2296.6 \angle 5.2583^\circ$. If a micro-PMU is used, then we can measure $\Delta V^d = 35.9 \angle 176^\circ$. If an ordinary RMS-value sensor is used, then we can measure $\Delta V^d = -35.5$.

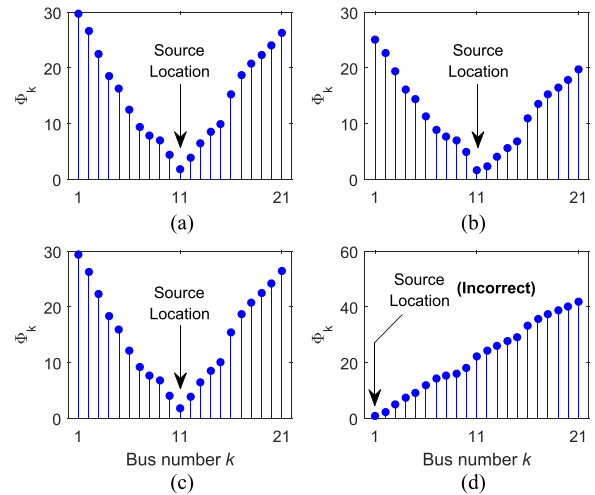


Fig. 8. Discrepancy measures for the cases in Section V-B. (a) Case A using micro-PMU data. (b) Case B using micro-PMU data. (c) Case A using RMS-value sensor data. (d) Case B using RMS-value sensor data.

- *Case B:* A 80 kW - 40 kVAR load is switched on at bus 11. This results in $V_{pre}^d = 2332.1 \angle 5.1183^\circ$ and $V_{post}^d = 2331.2 \angle 5.8693^\circ$. If a micro-PMU is used, then we can measure $\Delta V^d = 30.6 \angle 97^\circ$. If an ordinary RMS-value sensor is used then we can measure $\Delta V^d = -0.9$.

The results of applying the ESLI algorithm are shown in Fig. 8. We can see that both sensors can correctly identify the location of the event in Case A. However, an ordinary RMS-value sensor can barely notice the event in Case B. Accordingly, it *cannot* help identify the location of the event, see Fig. 8(d). One must use data from micro-PMUs instead in order to identify the event in Case B. Also see Section VI.

C. Discrepancy Based on Magnitude vs. Phasor Comparison

As expressed in (11), the discrepancy index in our analysis is obtained by conducting a comparison between the two sets of differential voltage *phasors* obtained from the backward and forward steps, i.e., ΔV^f and ΔV^b . Alternatively, one may attempt to identify the location of the event by examining the intersection of the two curves that are formed by plotting the magnitude of the forward and backward differential voltages. As an example, consider the capacitor bank event (Case I in Section V-A), in which the pseudo-measurements are perturbed with some practical level of errors. In Fig. 9(a), the magnitude of the differential voltage in the forward nodal voltage calculation, i.e., $|\Delta V^f|$; as well as the magnitude of the differential voltage in the backward nodal voltage calculation, i.e., $|\Delta V^b|$, are plotted. We can see that the intersection between the two voltage curves occurs between buses 14 and 15. Such intersection is closer to bus 14; as it can be confirmed in the magnified portion of this figure. Therefore, bus 14 would be identified as the event bus if intersection-based method is used. However, the correct event bus in this example is bus 15.

The problem with the intersection-based method in this example is that it essentially relies only on the magnitude of the differential voltage and ignores their phasor characteristics. This issue can be better understood by using the curves in Fig. 9(b).

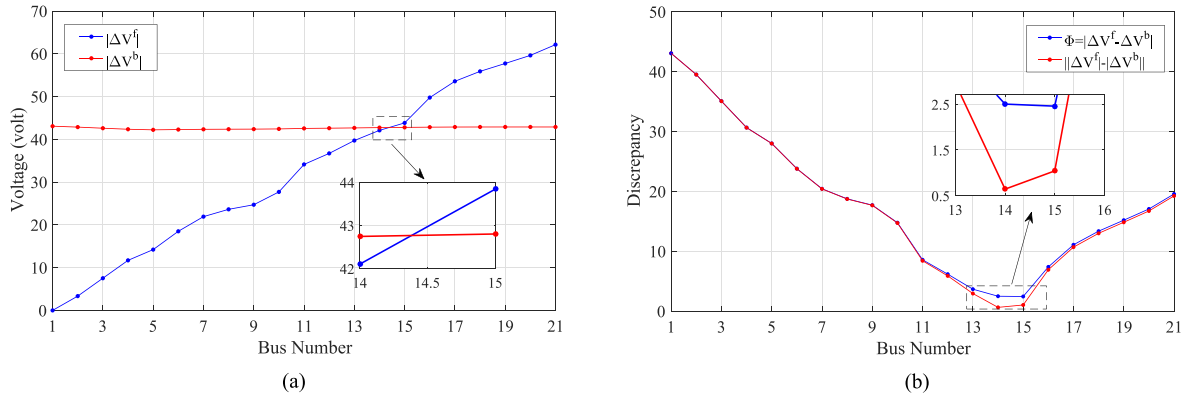


Fig. 9. The importance of calculating discrepancy based on phasors in case of a capacitor bank event location identification. (a) Incorrect identification of event location based on examining the intersection of differential voltage curves for voltage magnitude. (b) Comparing the differential voltage discrepancy curves based on voltage phasors, as in (11), versus magnitude only, as in (19).

TABLE I
SENSITIVITY ANALYSIS TO ERROR IN LINES IMPEDANCES

Error in Line Impedance (SD)	Correct Event Bus	Immediate Neighboring Bus	Another Bus	Max Error
5%	99.9%	0.1%	0%	1 bus
10%	89.7%	10.3%	0.02%	2 buses
15%	72.4%	26.0%	1.6%	3 buses
20%	59.2%	34.3%	6.5%	5 buses
25%	49.6%	36.7%	13.7%	5 buses

First consider the curve for

$$\left| |\Delta V^f| - |\Delta V^b| \right|. \quad (19)$$

The intersection-based method in the nodal calculation that we explained in the previous paragraph is equivalent to obtaining the minimum of the curve for the expression in (19). Such minimum would result in incorrectly identifying bus 14 as the event bus. Next, consider the curve for the proposed discrepancy index in (11). We can see that the minimum of this curve occurs at bus 15, which is the correct event bus.

Again, please pay attention to the magnified portion of the figure. The difference between the two approaches becomes evident by comparing (19) and (11), where the former is the discrepancy based on magnitude only; while the latter is the discrepancy based on phasors. Obtaining such phasor-based discrepancy is in fact one of the advantages of using phasor measurements as opposed to RMS-based measurements.

D. Analysis of Sensitivity and Robustness

In practice, the utility's knowledge about system parameters is not perfect and measurements are not precise. Uncertainty varies for different types of parameters and measurements. Nevertheless, we can examine the robustness of the proposed ESLI algorithm against any given level of parameter inaccuracy. Here, we use the Monte Carlo approach to generate different scenarios based on the given level of parameter error.

1) *Errors in Distribution Lines Impedances:* Table I shows the results when there are errors in the supposedly known impedances of distribution lines. For line impedance errors with 5% standard deviation (SD), nearly 99.9% of the event source locations are identified correctly. Even in those 0.1% of the cases where the event source is located incorrectly, the identified lo-

TABLE II
SENSITIVITY ANALYSIS TO ERROR IN PSEUDO-MEASUREMENTS

Error in Power Injection (SD)	Correct Event Bus	Immediate Neighboring Bus	Another Bus	Max Error
20%	~100%	~0%	0%	1 bus
40%	98.3%	1.7%	0%	1 bus
60%	92.2%	7.8%	0%	1 bus
80%	84.6%	15.4%	0%	1 bus
100%	78.7%	21.3%	~0%	2 buses

cation is an *immediate neighboring bus* of the bus where the event occurs. As we increase the error, the results still demonstrate an overall satisfying performance in event source location identification. For an impedance error with 25% SD, which is beyond any normal level of error in practice, either the correct event bus itself or its immediate neighboring bus is identified in $49.6 + 36.7 = 86.3\%$ of the cases.

2) *Errors in Pseudo-Measurements:* A similar sensitivity analysis can be done with respect to the pseudo-measurements on background power injections, i.e., loads and distributed generations. Of course, this would be a concern only if the distribution system is *not* equipped with smart meters. The results are shown in Table II. We can see that, even with errors with as high as 100% SD, either the correct event bus or its immediate neighboring bus is identified almost all the time.

3) *Errors in Measurements:* In principle, two sources of error can be considered in the context of this paper: the error in the micro-PMU device itself; as well as the error in the instrumentation channel. The latter is associated with the errors due to the CTs, PTs, control cables, and burden at the input of the micro-PMU. Based on various field experience and given the fact that micro-PMUs have very high precision with typical accuracy at 0.01% in magnitude and 0.003° in angle [28]; it is only the error in the instrumentation channel that is of concern in practice and must be considered. Interestingly, the errors in instrumentation channel, especially for distribution-level PTs and CTs, are *large but stable*. It means that the instrumentation channel errors are roughly *constant* for consecutive measurements that are made over a short period of time. As a result, the *measurement differences* at the same location, such as ΔV and ΔI in this study, are *not* significantly affected by the instrumentation channel errors.

TABLE III
PERFORMANCE WITH MEASUREMENT 0.5-CLASS CT/PT AGAINST
DIFFERENT LOAD SWITCHING LEVELS

Load Switching (p.u.)	Correct Event Bus	Immediate Neighboring Bus	Another Bus	Max Error
5%	100%	0%	0%	0 bus
2%	100%	~ 0%	0%	1 bus
1%	97.3%	2.6%	0.1%	2 buses
0.5%	95.2%	4.5%	0.3%	2 buses

TABLE IV
PERFORMANCE WITH PROTECTION 3-CLASS CT/PT AGAINST
DIFFERENT FAULT LEVELS

Fault Impedance	Correct Event Bus	Immediate Neighboring Bus	Another Bus	Max Error
5 Ω	100%	0%	0%	0 bus
10 Ω	100%	~0%	0%	1 bus
50 Ω	98.3%	1.7%	0%	1 bus
100 Ω	96.5%	3.3%	0.2%	2 buses

To discuss the effectiveness of the proposed method against the measurement errors, two scenarios are examined in this section to identify the location of a non-fault event and that of a fault event. It is assumed that the CTs/PTs used for non-fault events are of Measurement 0.5-Class; and the CTs/PTs used for fault events are of Protection 3-Class. In both scenarios, micro-PMUs are assumed to have their typical manufacturer-reported accuracy at 0.01% in magnitude and 0.003° in angle.

The results associated with the non-fault and fault events are shown in Table III and Table IV, respectively. These results demonstrate the effectiveness of our method against typical errors in measurements. In particular, when it comes to *major events* such as a 5% load switching (Table III) or a low-impedance fault with resistance 5 Ω (Table IV), the measurement errors do not at all influence the accuracy of event location identification. However, when it comes to *minor events* such as a 0.5% load switching (Table III) or a high-impedance fault with resistance 100 Ω (Table IV), the measurement errors may slightly affect the performance, because such minor events cause only very small variations in measurements which could be comparable with measurement error.

4) *Event Significance*: If an event is very small, then our method may no longer be able to identify the event location; because the information for such event could be lost within the errors in measurements. However, one may ask: do we really need to identify the location of such minor events? Nevertheless, it is reasonable to examine how the accuracy of the results are affected based on the size of the event. Table V shows the efficiency of our method for various events which cause different voltage and power variations. The error in measurement in each scenario is given based on the percentage error in magnitude and the actual degree error in phase angle. As can be seen, the reliable margin of measurements variation for running the proposed method depends on the accuracy of the micro-PMUs. The margin of measurement variations decreases as we improve the accuracy of micro-PMUs.

E. Performance Comparison

In this section, we compare the performance of our method with that of a method that works based on state estimation,

which is inspired by [18]. In order to have a fair comparison, we applied both our method and the state estimation-based method to the same practical test scenario, where both methods have access to live data only from two micro-PMUs to pin point the location of cap bank switching (Case I in Section V.A) among buses 1 to 21, as shown in Fig. 4. As it is shown in Fig. 6(a), our proposed method can efficiently localize this event, where two micro-PMUs are installed at buses 1 and 21.

As for the method based on state estimation that is used for comparison, the location of an event is determined based on the residuals obtained from state estimation. The residuals show the difference between pre-event and post-event power injections at different buses. The bus with the highest residual, i.e., the highest power injection difference, is determined as the location of the event. The results obtained from the state estimation-based method are shown in Fig. 10(a). To consider a fair comparison, we assume that two micro-PMUs are installed at buses 7 and 14 to divide the buses into three equal groups, which appeared to work the best for the state estimation method with two micro-PMUs. We can see that the highest residuals are associated with an array of buses from bus 15 to bus 21, which means that the state estimation-based method was able to only very roughly identify the overall region of the event, but not the actual location of the event.

The efficiency of the state estimation-based method is further appraised by increasing the number of micro-PMUs installations from two to four, at buses 4, 8, 12, and 16. The results are shown in Fig. 10(b). We can see that the highest residuals are associated with buses 12, 13, 14, 15, i.e., those buses that are located in between the two micro-PMUs at buses 12 and 16. We conclude that the state estimation-based method in this example can again loosely determine the overall region of the event, but not the exact location of the event. Ultimately, in order to precisely localize the event, *all* the buses are assumed to be equipped with micro-PMUs. The results are shown in Fig. 10(c). In contrast, our method can identify the location of the event with only two micro-PMUs.

VI. CASE STUDIES: PART II - REAL-LIFE NETWORK

In this section, we evaluate the performance of our proposed method using micro-PMU data from a real-life distribution feeder in Riverside, CA. The schematic diagram of this feeder is shown in Fig. 11. The actual GIS diagram of the feeder is also available in [6, Fig. 4]. This feeder is operated by Riverside Public Utilities (RPU), see <http://www.riversideca.gov>.

The under-study feeder includes multiple capacitor banks. On particular interest in this case study is a three-phase switched capacitor bank rated at 900 kVAR at bus 31, see Fig. 11. The capacitor bank is switched by a vacuum circuit breaker which is controlled by a Volt-VAR controller. This capacitor bank is *not* monitored by any sensor. Therefore, RPU is *not* aware of how the capacitor bank operates on a daily basis.

This feeder is also equipped with *two* micro-PMUs at buses 1 and 26. Fig. 12 shows the voltage and current phasors that are measured by the two micro-PMUs during a capacitor bank *switching on* event. This event can be detected by looking into the changes in the power factor of the distribution feeder as seen by micro-PMU 1, see [4] for more details. Other event detection methods may also be used, e.g., see [24], [25].

TABLE V
PERFORMANCE FOR DIFFERENT EVENT STRENGTHS AND DIFFERENT MEASUREMENT ERRORS

Event (% MVA base)	ΔS (MVA)	ΔV (Volt)	Error in Measurement (Magnitude/Angle)			
			(0.01%, 0.003°)	(0.025%, 0.006°)	(0.05%, 0.01°)	(0.1%, 0.02°)
0.5%	20	6	95.2	93.6	80.8	51.2
1%	40	12	97.3	95.3	93.7	81.2
2%	80	24	100	96.2	95	93.7
5%	200	62	100	100	97.6	94.9
10%	400	126	100	100	100	97.8

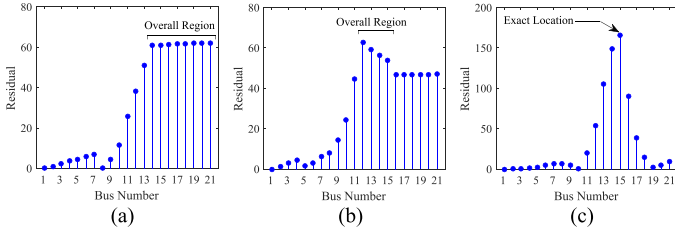


Fig. 10. The results associated with the state estimation-based method in [18] that is presented for performance comparison. (a) Two micro-PMUs are installed at buses 7 and 14. (b) Four micro-PMUs are installed at buses 4, 8, 12, and 16. (c) All the buses are equipped with micro-PMUs.

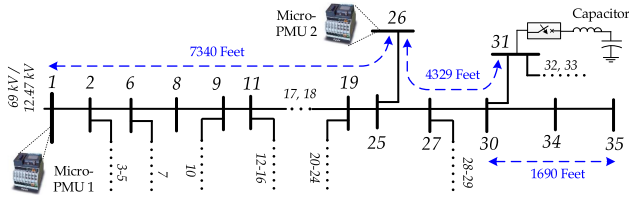


Fig. 11. Representation of a distribution feeder based on compensation theorem equivalent circuit. Measurements are done by two micro-PMUs.

At first glance, the data from micro-PMU 2 does *not* seem to provide any additional information, other than mimicking the voltage magnitude at substation. However, the use of micro-PMU 2 is critical to obtain the *location* of the capacitor. The results are shown in Fig. 13(a), where the event source is located correctly. Here, the MST buses are 1, 2, 6, 8, 9, 11, 17, 18, 19, 25, and 26. Therefore, as far as the information available to the two micro-PMUs is concerned, the correct event source location is bus 25. Buses 27 to 35 are the laterals of MST bus 25. Therefore, the source of the event should be sought at these buses; or bus 25 itself. According to the further information regarding the extent and nature of the capacitor bank event described in [4], it can be concluded that a capacitor bank is switched at bus 31, because bus 31 is the only bus with a capacitor bank on this lateral. Of course, it would have been better for the purpose of the analysis in this paper if micro-PMU 2 was installed at bus 35, i.e., at the end of the lateral. In that case, the ESLI method would identify bus 30 as the event source location.

It is worth noting that if we use only the magnitudes but not the phase angles of the micro-PMU measurements, i.e., as in RMS sensors, then bus 19 would be identified as the event source location, *which is incorrect*. Therefore, it is necessary to use micro-PMUs as opposed to RMS-based sensors.

The ESLI method can correctly identify also the location of the capacitor bank *switching off* event, as shown in Fig. 13(b).

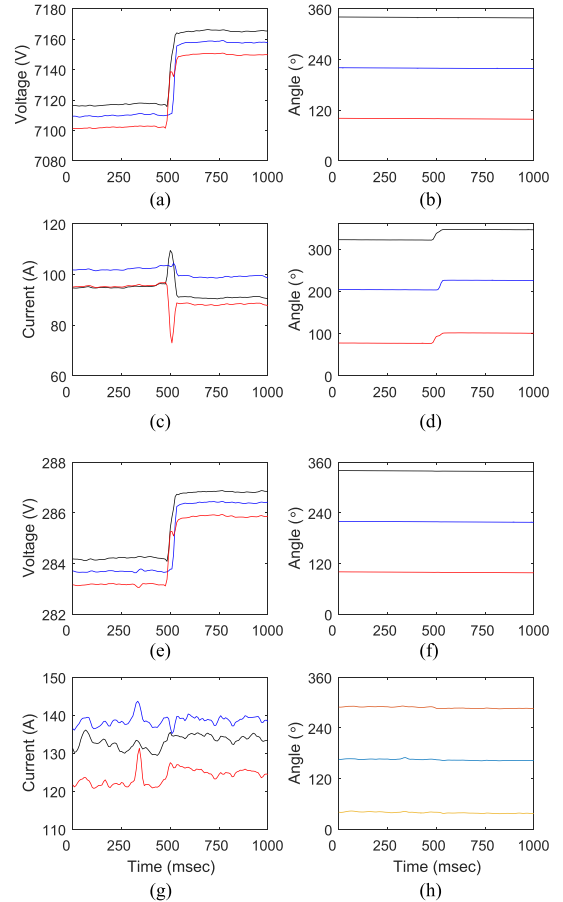


Fig. 12. A real-life capacitor bank *switching on* event. (a)–(d) Measurements from micro-PMU 1. (e)–(h) Measurements from micro-PMU 2.

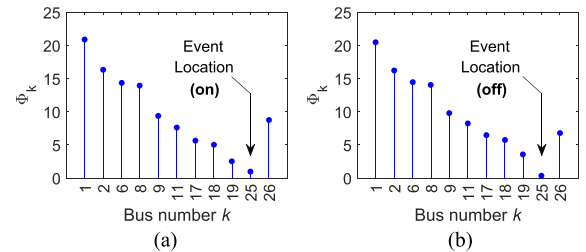


Fig. 13. Results for identifying the locations of capacitor bank switching events using real-world micro-PMU data. (a) Switching ON. (b) Switching OFF.

VII. POSSIBLE LIMITATIONS OF THE PROPOSED METHOD

The potential limitation and challenges for the ESLI method implementation can be described as follows:

Significance of the Event: While the theory in this paper is valid regardless of the significance of the event; in practice, if the event is too small, e.g., there is only a very minor change in impedance, then the location of the event may not be identified correctly due to the presence of measurement errors or lack of updated pseudo-measurements. Although, this limitation may not have major impact in practice, because if the event is indeed minor, then it may not be of interest to be scrutinized.

Number of Micro-PMUs: The proposed method can precisely determine the location of events when they occur on MST buses; otherwise, the MST bus that is closest to the true event bus will be identified. In this regard, if all we need is to know the lateral where the event is located, then we can obtain the acceptable results by using only two micro-PMUs, one at the substation and one at the end of the feeder. However, if the exact location of the event on a lateral is important then we also need micro-PMU installations at the end of the laterals.

Pre-Event and Post-Event Stability: Our proposed method is intended to localize *stable* events. That is, for our method to work properly, the network should be in its stable mode both before and after the event. This is because we essentially use steady-state pre-event and post-event measurements.

Changes in System Frequency: In practice, the system frequency often deviates from the nominal system frequency, e.g., 60 Hz in North America. If such deviations in frequency are significant, then they can potentially affect the estimated angle of phasor measurement. These changes for a short period of time follow a quasi-steady rate which is called the rate of change of frequency (ROCOF). Therefore, to find the true change in phase angle following an event, the ROCOF should be taken into account. Therefore, as a future research direction, one may consider the performance of our method - or the performance of any method based on micro-PMUs for that matter - during the major system-wide frequency events.

VIII. CONCLUSION

A novel application of micro-PMUs is proposed, based on an innovative use of the compensation theorem in circuit theory, to identify the location of events in power distribution systems. At least two micro-PMUs must be installed in order to implement this method, one at the substation and another one at the end of the feeder. However, based on the importance of buses, additional micro-PMUs can be deployed at the end of laterals to make the buses on laterals observable. Simulation results on an IEEE 123 test system showed that the proposed method can accurately estimate the exact location of different types of events, including power quality events, faults, as well as events that are benign yet they can reveal how different components operate across the feeder. Since the proposed method is based on measurement differences, it has a reasonably robust performance with respect to measurement errors. The performance is robust also against errors in pseudo-measurements as well as in distribution lines impedances. The importance of using phase angle measurements was shown analytically and also through cases studies; thus, justifying the use of micro-PMUs as opposed to ordinary RMS-based voltage and current sensors. The effectiveness of the proposed method is confirmed also by using micro-PMU measurements from a pilot real-life distribution feeder in Riverside, CA.

APPENDIX

The polynomial load model is widely used in power system studies. This model consists of three main parts: constant-impedance, constant-current, and constant-power. Accordingly, the injection current at bus i can be described as:

$$I_i = I_i^Z + I_i^I + I_i^P, \quad (20)$$

where I_i^Z , I_i^I , and I_i^S denote the injection current at bus i associated with the constant-impedance, constant-current, and constant-power load components, respectively. Once we replace the electrical model associated with each load component, we can rewrite (21) as:

$$I_i = Y_i V_i + C_i^I + \left(\frac{C_i^S}{V_i} \right)^*, \quad (21)$$

where V_i is the voltage at bus i ; and $*$ denotes the conjugate operator. Parameters Y_i , C_i^I , and C_i^S are associated with load admittance in the constant-impedance model, quantity of current in the constant-current model, and apparent power in the constant-power model. The variation of I_i can now be expressed with respect to the variation of V_i :

$$\Delta I_i = Y_i \Delta V_i + C_i^{S*} \left(\frac{1}{V_i^{\text{pre}} + \Delta V_i} - \frac{1}{V_i^{\text{pre}}} \right)^*. \quad (22)$$

The above expression describes the relationship between ΔI_i and ΔV_i once all the load types are taken into account. Throughout the formulations in this paper, we use the constant-impedance model, where ΔI_i is obtained from the production $Y_i \Delta V_i$. As for the constant-power model, the deviation in injection current can be obtained from the second term in (22). For the constant-current model, the load has the same current before and after the change in the network. As a result, the injection current deviation derived from constant-current loads is zero, i.e., constant-load model can be ignored.

Once all the load types are considered, the relationship in (22) can be integrated into the forward and backward nodal voltage calculations in (6) and (8), i.e., ΔI_i^f in (6) and ΔI_i^b in (8) can be obtained from (22). Of course, this will make (6) and (8) longer and more complicated to present. However, just like the analysis in Section II, the updated formulations of (6) and (8) would be correct at all buses, *except for* bus k , in which the event occurs. Accordingly, the classification in (8) and the rest of the analysis will remain unchanged.

REFERENCES

- [1] H. Mohsenian-Rad, E. Stewart, and E. Cortez, "Distribution synchrophasors: Pairing big data with analytics to create actionable information," *IEEE Power Energy Mag.*, vol. 16, no. 3, pp. 26–34, May/Jun. 2018.
- [2] A. von Meier, E. Stewart, A. McEachern, M. Andersen, and L. Mehrmanesh, "Precision micro-synchrophasors for distribution systems: A summary of applications," *IEEE Trans. Smart Grid*, vol. 8, no. 6, pp. 2926–2936, Nov. 2017.
- [3] O. Samuelsson, M. Hemmingsson, A. H. Nielsen, K. O. H. Pedersen, and J. Rasmussen, "Monitoring of power system events at transmission and distribution level," *IEEE Trans. Power Syst.*, vol. 21, no. 2, pp. 1007–1008, May 2006.

- [4] A. Shahsavari *et al.*, "A data-driven analysis of capacitor bank operation at a distribution feeder using micro-PMU data," in *Proc. IEEE Power Energy Soc. Innovative Smart Grid Technol. Conf.*, Washington, DC, USA, Apr. 2017, pp. 1–5.
- [5] M. Jamei *et al.*, "Micro synchrophasor-based intrusion detection in automated distribution systems: Toward critical infrastructure security," *IEEE Internet Comput.*, vol. 20, no. 5, pp. 18–27, Sep./Oct. 2016.
- [6] A. Shahsavari *et al.*, "Distribution grid reliability versus regulation market efficiency: An analysis based on micro-PMU data," *IEEE Trans. Smart Grid*, vol. 8, no. 6, pp. 2916–2925, Nov. 2017.
- [7] A. Sadeghi-Mobarakeh, A. Shahsavari, H. Haghghat, and H. Mohsenian-Rad, "Optimal market participation of distributed load resources under distribution network operational limits and renewable generation," *IEEE Trans. Smart Grid*, to be published, doi: [10.1109/TSG.2018.2830751](https://doi.org/10.1109/TSG.2018.2830751).
- [8] H. Mohsenian-Rad, V. Wong, J. Jatskevich, R. Schober, and A. Leon-Garcia, "Autonomous demand-side management based on game-theoretic energy consumption scheduling for the future smart grid," *IEEE Trans. Smart Grid*, vol. 1, no. 3, pp. 320–331, Dec. 2010.
- [9] Institute of Electrical and Electronics Engineers, *IEEE Guide for Collecting, Categorizing, and Utilizing Information Related to Electric Power Distribution Interruption Events*, *IEEE Std 1782-2014*, Aug. 2014.
- [10] D. Arnold, C. Roberts, O. Ardakanian, and E. Stewart, "Synchrophasor data analytics in distribution grids," in *Proc. IEEE Power Energy Soc. Innovative Smart Grid Technol. Conf.*, Washington, DC, USA, Apr. 2017, pp. 1–5.
- [11] A. Shahsavari, M. Farajollahi, E. Stewart, C. Roberts, and H. Mohsenian-Rad, "A data-driven analysis of lightning-initiated contingencies at a distribution grid with a PV farm using micro-PMU data," in *Proc. IEEE Power Symp. NAPS*, Morgantown, WV, USA, Sep. 2017, pp. 1–6.
- [12] M. Farajollahi, A. Shahsavari, and H. Mohsenian-Rad, "Location identification of distribution network events using synchrophasor data," in *Proc. IEEE Power Symp. NAPS*, Morgantown, WV, USA, Sep. 2017, pp. 1–6.
- [13] M. Farajollahi, A. Shahsavari, and H. Mohsenian-Rad, "Tracking state estimation in distribution networks using distribution-level synchrophasor data," in *Proc. IEEE PES GM*, Portland, OR, USA, Aug. 2018, pp. 1–5.
- [14] M. Farajollahi, A. Shahsavari, and H. Mohsenian-Rad, "Location identification of high impedance faults using synchronized harmonic phasors," in *Proc. IEEE Power Energy Soc. Innovative Smart Grid Technol. Conf.*, Washington, DC, USA, Apr. 2017, pp. 1–5.
- [15] R. Krishnathar and E. E. Ngu, "Generalized impedance-based fault location for distribution systems," *IEEE Trans. Power Del.*, vol. 27, no. 1, pp. 449–451, Jan. 2012.
- [16] J. Ren, S. Venkata, and E. Sortomme, "An accurate synchrophasor based fault location method for emerging distribution systems," *IEEE Trans. Power Del.*, vol. 29, no. 1, pp. 297–298, Feb. 2014.
- [17] M. Majidi, M. Etezadi-Amoli, and M. S. Fadali, "A novel method for single and simultaneous fault location in distribution networks," *IEEE Trans. Power Syst.*, vol. 30, no. 6, pp. 3368–3376, Nov. 2015.
- [18] M. Pignati, L. Zanni, P. Romano, R. Cherkaoui, and M. Paoletti, "Fault detection and faulted line identification in active distribution networks using synchrophasors-based real-time state estimation," *IEEE Trans. Power Del.*, vol. 32, no. 1, pp. 381–392, Feb. 2017.
- [19] D. J. Won, I. Y. Chung, J. M. Kim, S. I. Moon, J. C. Seo, and J. W. Choe, "A new algorithm to locate power-quality event source with improved realization of distributed monitoring scheme," *IEEE Trans. Power Del.*, vol. 21, no. 3, pp. 1641–1647, Jul. 2006.
- [20] K.-R. Shih and S.-J. Huang, "Application of a robust algorithm for dynamic state estimation of a power system," *IEEE Trans. Power Syst.*, vol. 17, no. 1, pp. 141–147, Feb. 2002.
- [21] Y. Seyedi, H. Karimi, and S. Grijalva, "Distributed generation monitoring for hierarchical control applications in smart microgrids," *IEEE Trans. Power Syst.*, vol. 32, no. 3, pp. 2305–2314, May 2017.
- [22] A. Eshraghi and R. Ghorbani, "Islanding detection and over voltage mitigation using controllable loads," *Sustain. Energy, Grids Netw.*, vol. 6, pp. 125–135, Feb. 2016.
- [23] K. S. Kumar, *Electric Circuits and Networks*. Taramani, India: Pearson, 2009.
- [24] M. Jamei *et al.*, "Anomaly detection using optimally-placed μ pmu sensors in distribution grids," *IEEE Trans. Power Syst.*, vol. 33, no. 4, pp. 3611–3623, Jul. 2018.
- [25] Y. Zhou, R. Arghandeh, and C. J. Spanos, "Partial knowledge data-driven event detection for power distribution networks," *IEEE Trans. Smart Grid*, vol. 9, no. 5, pp. 5152–5162, Sep. 2018.
- [26] Y. Xiao, J.-C. Maun, H. Mahmoud, T. Detroz, and S. Do, "Harmonic impedance measurement using voltage and current increments from disturbing loads," in *Proc. 9th Int. Conf. Harmonics Quality Power*, Orlando, FL, USA, Oct. 2000, vol. 1, pp. 220–225.
- [27] Radial distribution Test Feeders, Distribution System Analysis Subcommittee Rep., 2017. [Online]. Available: <http://ewh.ieee.org/soc/pes/dsacom/testfeeders.html>
- [28] "Micro-pmu data sheet," 2017. [Online]. Available: <https://www.powerstandards.com/download-center/micropmu/>



Mohammad Farajollahi (S'15) received the B.Sc. degree in electrical engineering from the University of Tehran, Tehran, Iran, in 2014, the M.Sc. degree in electrical engineering from the Sharif University of Technology, Tehran, Iran, in 2016, and is currently working toward the Ph.D. degree with the University of California, Riverside, CA, USA. His research interests include power system planning, operation, reliability, as well as optimization. He is specifically working on applications of micro-PMUs and data analysis in distribution system monitoring.



Alireza Shahsavari (S'17) received the M.Sc. degree in electrical engineering—Power systems from the University of Tehran, Tehran, Iran, in 2013. He is currently working toward the Ph.D. degree in electrical and computer engineering with the University of California, Riverside, CA, USA. He was the recipient of Best Master Thesis National Award, Iran, 2014. His research interests include the data analysis in power systems and smart grid, distribution system planning and operation, and power system reliability.



Emma M. Stewart (M'08–SM'14) received the undergraduate degree in electrical and mechanical engineering from the University of Strathclyde, Glasgow, U.K., in 2004, and the Ph.D. degree in electrical engineering in 2009. She joined BEW Engineering in 2009, and held the position of Senior Engineer in the Transmission and Distribution team, where she led distribution studies for interconnection and high renewable penetration studies for large utilities. Dr. Stewart joined Lawrence Berkeley National Laboratory in 2009, and was the Deputy Group Leader for grid integration. She joined the Global Security team with Lawrence Livermore National Laboratory, and is the Deputy Associate Program Leader for Infrastructure Systems.



Hamed Mohsenian-Rad (S'04–M'09–SM'14) received the Ph.D. degree in electrical and computer engineering from the University of British Columbia, Vancouver, BC, Canada, in 2008. He is currently an Associate Professor of electrical engineering with the University of California, Riverside, CA, USA. His research interests include modeling, data analysis, and optimization of power systems and smart grids. He was the recipient of the National Science Foundation CAREER Award, the Best Paper Award from the IEEE Power and Energy Society General Meeting, and the Best Paper Award from the IEEE International Conference on Smart Grid Communications. He was an Editor of the IEEE TRANSACTIONS ON SMART GRID and the IEEE POWER ENGINEERING LETTERS.